A new designed for disassembly shear connection for steel-timber composite beams

José Henriques[a], Pibbe Willems[b], Alper Turgut[a], Ellen Maerten[a], Liselotte De Ligne[b] and Hervé Degée[a]

[a] *Construction Engineering Research Group, Faculty of Engineering Technology, University Hasselt, Belgium*
[b] *Laboratory of Wood Technology (UGent-Woodlab), Department of Environment, Faculty of Bioscience Engineering, Ghent University, Belgium*

Abstract: This paper presents a newly developed shear connection for steel–timber composite (STC) floor beams. The connection's mechanical behaviour is investigated through experimental tests, including push-out tests and hygroscopic assessments, which are used to determine the load–slip response, identify the governing failure mode, and evaluate the effects of dimensional changes in wood. Finite element method (FEM) simulations are then conducted to reproduce the connection behaviour numerically. Finally, a component-based method is proposed to determine the shear connection properties, including stiffness and strength, and to assess its efficiency through comparison with conventional dowel-type connections.

1. Introduction

Steel–timber composite (STC) structures have emerged over the past decade as a response to the construction sector's urgent need to reduce its environmental impact and make better use of available resources. For the steel construction industry, the development of high-performance Engineered Wood Products (EWPs), combined with their environmentally friendly properties, presents an opportunity to reduce reliance on reinforced concrete. In the case of building floors and decks, the combination of steel and EWP panels offers competitive solutions with a lower environmental footprint. The inherent characteristics of these two materials also enable dry construction methods and allow for extensive prefabrication, including the use of automation in the production process. This prefabricated approach supports the principles of a circular economy by extending the life cycle of construction elements and facilitating the reuse of materials.

In STC floor beams, the shear connection between materials plays a crucial role. Both structural performance and the ease of execution, including on-site assembly, depend heavily on the type of connection used. Over the past decade, various shear connection systems have been developed [1]-[5], including: i) Dowel-type connections, such as screws or bolts, with or with-

out preloading; ii) Adhesive-type connections, such as bonded-in steel connectors, with or without dowel reinforcement; iii) Contact-type connections, such as post-tensioned bolts with grout. Among these, dowel-type connections using non-preloaded bolts or screws are the most common. While they are simple to assemble, their flexible behaviour results in significant nonlinear deformation even under low level of load. This leads to non-negligible slip at the material interface, which reduces composite action, and eventual permanent deformations in the EWP panels, potentially hindering their reuse in circular construction. Alternative solutions can mitigate these drawbacks. However, they often require greater execution effort (e.g., gluing or preloading), restrict disassembly, or remain insufficiently studied to fully assess the effects of time-dependent behaviour (e.g., preloaded connections). Consequently, the development of new shear connection systems is still needed, namely, ones that can simultaneously ensure efficient structural performance and compatibility with circular economy principles, particularly regarding ease of assembly and disassembly.

This paper introduces a new reversible shear connection for high-performance circular STC floor beams, currently being developed and investigated within the CIRCOMP project [6]. The concept of the connection is first described, including its execution steps and load-transfer mechanisms. The mechanical behaviour is then characterized through push-out and hygroscopic tests, the latter assessing the effects of restrained dimensional variations within the EWP panel. A preliminary numerical model is subsequently presented to complement the experimental program and is partially validated. Finally, an analytical component-based model is proposed to determine the key mechanical properties of the shear connection, namely slip stiffness and strength.

2. Conceptual development of new reversible shear connection for STC

The development of a new reversible shear connection for STC floor beams originates from the limitations identified in existing solutions: i) mechanically flexible connections that restrict composite action; ii) systems that are complex to execute and not designed with circular construction in mind, such as glued connections, grout-based systems, or preloaded fasteners. To address these issues, inspiration was drawn from timber–concrete composite (TCC) floor beams, a field with decades of research and development [7]. In TCC systems, notched connections are known to provide high initial slip stiffness (enhancing composite action) and high load-bearing capacity, although exhibiting limited ductility. While ductility is generally desirable, its absence may be less critical in this context. Ductility can be provided by other structural components, and when aiming for circular use and extended material lifespans, ultimate limit states based on failure may need to be reconsidered (a topic beyond the scope of this paper). Building on this, a notched-inspired solution was adopted for the design of a new reversible shear connection for STC floor beams. The system consists of: i) The connector: a steel block with countersunk holes for screws (to fix it to the EWP panel) and threaded holes for bolts (to attach it to the steel beam) (Fig. 1-a); ii) The EWP panel: manufactured with grooves to accommodate the connectors (Fig. 1 -b); iii) The steel beam: fabricated with standard holes allowing bolts to pass through and fix the connector to the flange (Fig. 1-c). The execution process is foreseen as follows: i) The connector is attached to the EWP panel with screws, preferably in the factory; ii) On site, the EWP panel is fixed to the steel beam with bolts tightened by hand, without preloading. Standard execution tolerances for both materials should be applied to ensure ease of assembly. The assemble STC beam is illustrated in Fig. 1-d). The load-transfer mechanism may be described as follows: i) The shear load is primarily resisted through mechanical interlock (contact) between the EWP panel and the connector; ii) Screws are engaged until contact is achieved, with their main function being to prevent separation — hence, pull-

out resistance is required; iii) Between the steel beam and the connector, load transfer occurs through bolt–flange bearing action.

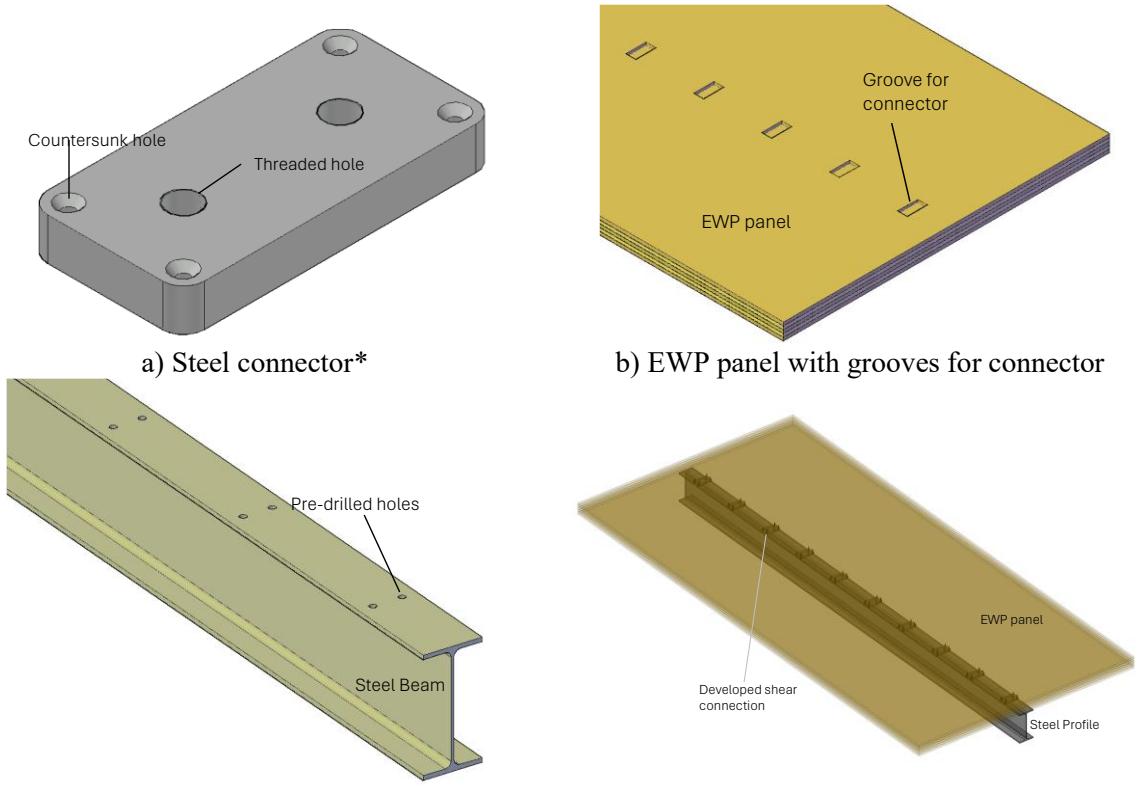

a) Steel connector* b) EWP panel with grooves for connector

c) Steel beam with predrilled holes d) STC beam assembly

Fig. 1: New reversible shear connection for STC floor beams

*A patent application related to this connector is currently pending.

3. Experimental characterization

3.1 Experimental program

The experimental program includes two types of tests: i) mechanical tests, consisting of push-out tests; ii) hygroscopic tests, carried out in a climate chamber.

To determine the load–slip response of the shear connection, symmetric push-out tests were conducted, as illustrated in Fig. 2, at the Application Centre Concrete and Construction (ACB^2) of Hasselt University. At this stage, only a reference configuration was tested; no geometric or material variations were considered. Since the primary unknown is the mechanical interlock strength, the specimens were designed to fail through local timber crushing. Table 1 summarizes the main geometric and material properties. As the material characterization tests have not yet been completed, nominal values are reported at this stage. The monitoring system used to obtain the load–slip behaviour (see Fig. 2) consisted of: i) a load cell; ii) four LVDTs (two on each side) measuring relative displacement between the steel profile and EWPs in the load direction; iii) two LVDTs (one on each side) measuring material separation. A total of five specimens were tested under short-term quasi-static loading. For four of them, the loading procedure followed EN 26891 [8], with one loading–unloading cycle between 10% and 40% of the estimated load. For one specimen, ten loading–unloading cycles within the same load range were applied to assess potential property degradation due to cyclic loading.

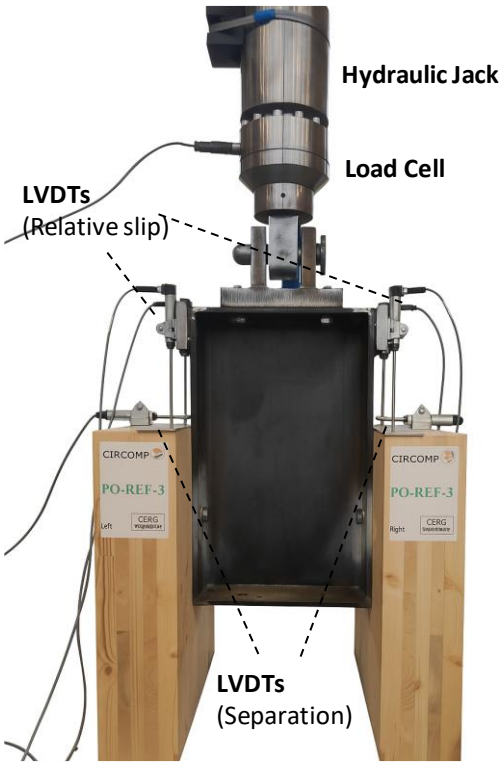

Fig. 2: Illustration of test specimen with test setup and monitoring

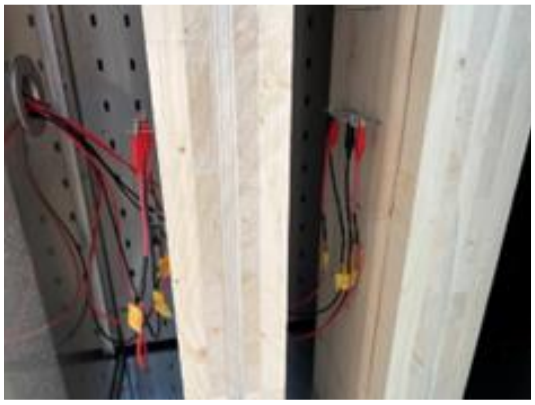

Fig. 3: Continuous measurement of steel-timber connection in climate chamber

Table 1: Geometrical and material properties of test specimens used in the mechanical tests

CLT	Steel Profile	Connector	Bolts	Screws
t = 120 mm (30/20/20/20/30) h = 500 mm b = 400 mm Wood Class, C24	IPE 300 h = 500mm Grade, S355	t = 20 mm l = 50 mm b = 140 mm Grade, S355	M16 Grade 8.8	d = 5 mm Paneltwistec SK AG Eurotec® ETA-11/0024

t – thickness, h – height, b – width, l – length, d - diameter

The behaviour of wood under indoor conditions was evaluated using a humidity cycling test (HCT), as shown in Fig. 3. The test specimen consists of a CLT panel connected to a steel using three connectors with 500mm spacing. The geometrical and material properties of the test specimen used in the hygroscopic tests are summarized in Table 2. Three humidity cycles were performed at 20 °C, with relative humidity (RH) varying from 35% → 65% → 90%, and specimens exposed for 168 hours (1 week) at each RH level in a climate cabinet (CTS, Clima Temperatur Systeme, CP 10/1100). After these cycles, a drying phase at approximately 68% RH and 20 °C was applied in a climate chamber, followed by final oven drying at 103 °C for 68 hours. Moisture content (MC) was monitored using both the electronic resistance method and the gravimetric method. For the electronic resistance method, insulated stainless steel nails were inserted at connector positions, and MC was recorded continuously with a Scanntronic Gigamodule. Additional readings were taken after each cycle and this at four extra points with a GANN Hydromette HT 85T to capture local variations. The gravimetric method provided averaged MC values for calibration and verification. Dimensional changes and crack development were assessed by marking measurement points and taking photographs of all specimens faces under consistent conditions. Height measurements were taken with a calliper aligned along premarked vertical reference lines on the end grain, ensuring consistent positioning, while width measurements were carried out using a custom measurement aid consisting of two wooden

plates and a reference nail to maintain repeatable alignment. This methodology allowed tracking of both local and averaged moisture dynamics, as well as corresponding swelling and shrinkage.

Table 2: Geometrical and material properties of test specimens used in the mechanical tests

CLT	Steel Plate	Connector	Bolts	Screws
t = 120 mm (30/20/20/20/30) h = 1200 mm b = 400 mm Wood Class, C24	t = 10 mm h = 1200 mm b = 150 mm Grade, S355	t = 20 mm l = 50 mm b = 140 mm Grade, S355	M16 Grade 8.8	d = 5 mm Paneltwistec SK AG Eurotec® ETA-11/0024

3.2 Test results

3.2.1 Mechanical tests

The main mechanical properties obtained from the conducted tests are summarized in Table 3. These have been derived from the load-slip curves and are expressed as relative load-slip curves in Fig. 4. The reported results refer to the full test specimen, which consists of two connections, one on each side of the steel profile. The values reported in Table 3 are the following: i) load capacity (F_{max}); ii) secant stiffness in reloading cycle, determined between 10% and 40% of the F_{max} ($K_{10\text{-}40}$); iii) secant stiffness up to F_{max} ($K_{0\text{-}max}$); iv) ultimate slip (δ_u) equal to the slip corresponding to 90% of F_{max} in the post peak range. It should be noted that at this stage the experimental results are not yet fully processed. Therefore, the slip values also include system gaps; before engaging, the contact bolts must "travel" the entire hole clearance (2 mm). The load-slip behaviour can be divided in three stages, as shown in Fig. 4: i) *Stage 1*, Friction between the steel flange and connector (no preload was explicitly applied; bolts were hand-tightened), together with dowel action from the screwed connection, the latter mainly governs the deformation in this stage; ii) *Stage 2*, Once friction is overcome, the steel profile slips until the bolts engage in bearing against the steel profile; iii) *Stage 3*, The steel connector engages in contact with the timber, which becomes the dominant load-transfer mechanism between the two parts. The maximum load, which shows a relatively low coefficient of variation (CV), is governed by local crushing of the timber, further leading to crack development, as illustrated Fig. 5. The variation in load capacity between test specimens is mainly due to connector misalignments during installation in the CLT and local imperfections in the wood. Fig. 5 highlights the difference between specimens 1 and 2, representing the weakest and strongest specimens, respectively. Specimen 1 shows uneven contact between the connector and the wood, leading to local rotation and stress concentration. Next, the shear connection stiffness provided by the connector when the connector and wood develop mechanical interlock is significant, as expressed by the secant stiffness $k_{10\text{-}40}$. Then, in terms of slip capacity, the average value is approximately 13 mm. If the "free" slip is discounted, the value shown in Fig. 4 reduces it to about 10 mm. This falls within the limit required by EN 1994-1-1 [9] for a shear connection to be classified as ductile. Nevertheless, it remains considerably lower than what is typically observed in common dowel-type connections [2].

Table 3: Summary of main mechanical properties of the tested shear connections

	F_{max} [kN]	$K_{10\text{-}40}$ [KN/mm]	$K_{0\text{-}max}$ [KN/mm]	δ_u [mm]
Average	211,0	269,0	31,2,3	13,4
σ	20,3	14,6	1,45	2,2
CV	9,6%	5,4%	4,6%	16,6%

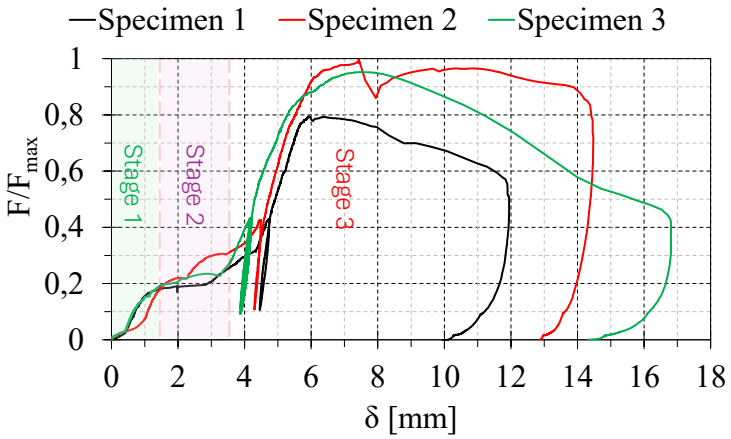

Fig. 4: Relative load – slip curve (F_{max} = 230,5kN)

a) Specimen 1 (lower load capacity) *

b) Specimen 2 (highest load capacity) *

Fig. 5: Failure pattern observed in the test specimens

*A patent application related to this connector is currently pending.

3.2.2 Hygroscopic tests

In the humidity cycling test (HCT) the moisture content (MC) of the wood showed consistent trends, as determined by both the electrical resistance method and the gravimetric method. At higher relative humidity, the MC increased, while during drying phases a decrease was observed. Wood absorbs moisture more quickly than it releases it, which is typical for the hygroscopic behaviour of the material. The electrical resistance method recorded local variations, whereas the gravimetric method provided a more uniform, averaged view of the MC. The maximum measured values were around 15% with the electrical resistance method and 12% according to the gravimetric measurements. Around the positions of the connectors, no significant moisture accumulation was observed, indicating limited moisture infiltration; however, this will be further verified using X-ray CT scans to confirm the findings.

The dimensional changes of the wood were consistent with the MC results, showing clear and rapid swelling at higher humidity levels, while the shrinkage process during drying occurred relatively more slowly. Changes thickness remained limited to approximately 2 mm, indicating a minor dimensional response of the wood under the tested conditions (Fig. 6). Width measurements showed smaller and less consistent changes of around 1 mm, suggesting that wood expands less in width than in height (Fig. 6). Measurement variability was higher, partly due to the larger dimensions of the specimens and the limited precision of the measurement method. During an initial visual inspection, no significant or problematic cracks were observed, even during extreme overdried phases. Further imaging analysis is planned to confirm these observations.

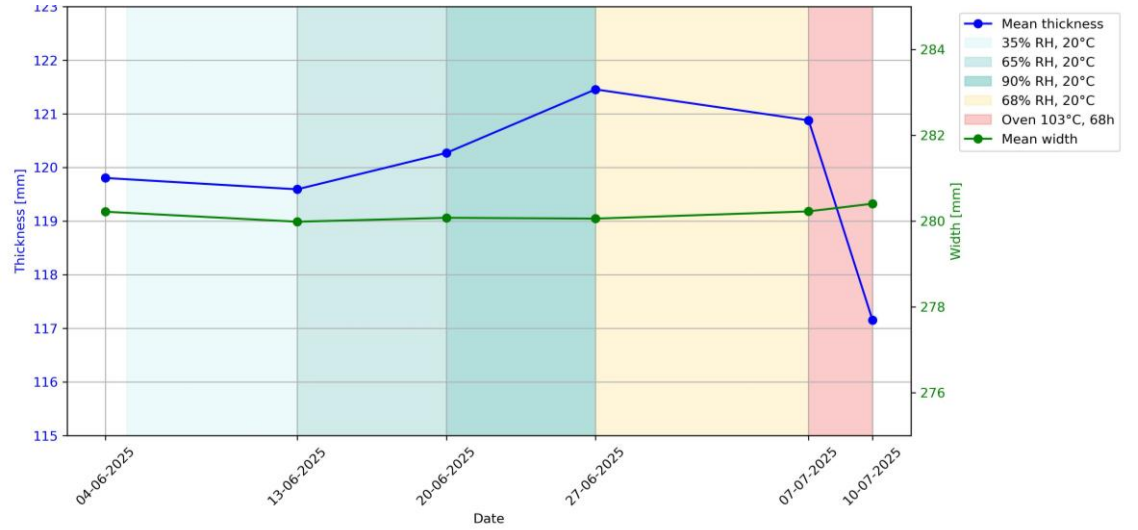

Fig. 6: Hygroscopic tests mean dimensional changes (thickness and width)

4. FEM numerical simulation

The numerical simulation used to reproduce the mechanical tests on the new reversible connection was developed in the general-purpose finite element method (FEM) software Abaqus [10]. At this stage, two preliminary models have been created, differing mainly in the material constitutive model adopted for the material wood. This is a critical issue. The anisotropic behaviour of the material, combined with its brittle yet relatively ductile response depending on stress type and orientation, poses significant challenges for such simulations. The main features of the developed models are as follows:

- Element type: All parts were explicitly modelled using solid finite elements with reduced integration available in the software library (C3D8R).
- Steel parts (profile, connector, bolts, screws, washers): modelled as elasto-plastic with isotropic strain hardening, based on nominal material properties.
- Wood: i) elastic orthotropic material (defining the engineering constants Ei, Gij, υij) with anisotropic yielding (Hill criterion [10]), hereafter referred to as FEM-Hill; ii) elastic orthotropic material (Ei, Gij, υij) with a user-defined subroutine (UMAT) to simulate brittle failure mechanisms (tension and shear), including damage initiation through the Damage Separation Model (DSM) approach [11], hereafter referred to as FEM-Damage.
- Interactions: i) screws–CLT with tie constraints (rigid link between element nodes), threads not explicitly modelled; ii) connector–CLT surface contact with soft contact behaviour in the normal direction and a penalty method in the tangential direction (friction coefficient 0.25); iii) all other mechanical interactions modelled with hard contact in the normal direction and a penalty method in the tangential direction (friction coefficient 0.25 for wood–steel contact, 0.4 for steel–steel contact).
- Symmetry: The model geometry was reduced to one quarter (symmetry conditions).
- Boundary and loading conditions: i) displacement of the CLT bottom constrained in all directions; ii) displacements normal to the symmetry planes constrained; iii) imposed displacement applied to the steel beam; iv) bolts and screws without preload.
- Nonlinear numerical solver: Newton method.
- Material and geometrical linearities: included.
- Geometrical imperfections: not included.

The developed numerical model is illustrated in Fig. 7-a). In Fig. 8, the relative load–slip curves compare the results of the numerical simulations with the experimental results. It should be noted that the actual gap observed in the tests was not modelled; therefore, the numerical results were shifted accordingly. From this comparison, the following can be observed: i) The Hill criterion leads to a clear overestimation of resistance and is unsuitable for such problems. In contrast, the user-defined constitutive model (UMAT) provides an accurate estimation of connection resistance (FEM/TEST = 1,08), despite the numerical model not accounting for imperfections. ii) Both models provide a good estimation of the elastic stiffness of the connection, as confirmed in the chart and further validated by the computed secant stiffness ($k_{10–40}$), which is 306,7 kN/mm for FEM-Hill and 298,4 kN/mm for FEM-Damage, remember values in Table 3. iii) In the post-peak stage, the FEM-Damage model requires further calibration, while the FEM-Hill model, as expected, fails to capture this behaviour since it assumes ductile response. In Fig. 7-b) is shown the high concentration of stresses (damage zone) showing a good correspondence with the observed damage in the experimental tests (see Fig. 5) above.

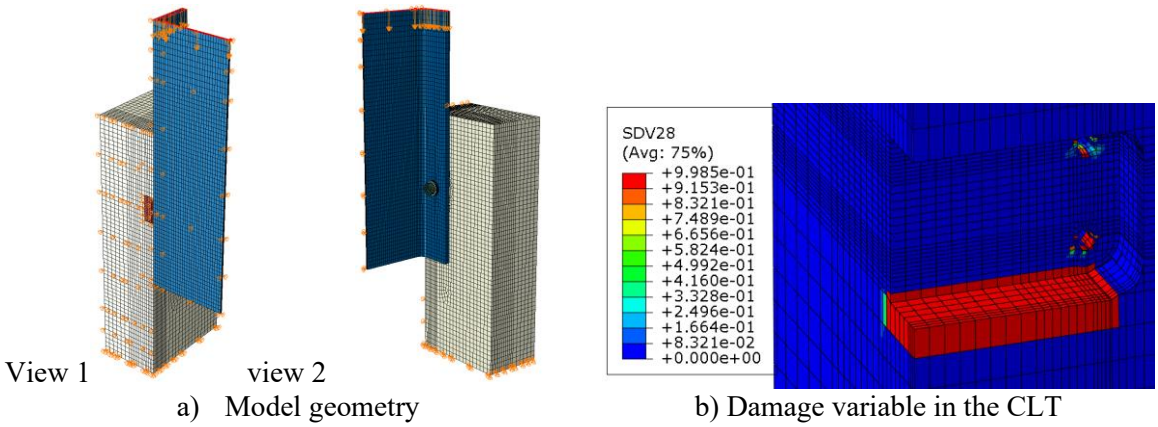

a) Model geometry b) Damage variable in the CLT

Fig. 7: FEM model of the push-out tests

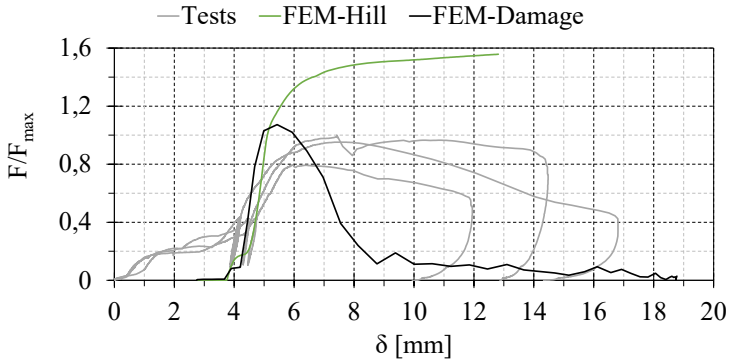

Fig. 8: Relative load-slip curves comparing FEM models and experimental tests

5. Analytical component-based model

In order to determine the load-bearing capacity of the newly developed connection under shear load, the component method principle is applied. Accordingly, the following connection components are identified and should be characterised (stiffness and strength): i) Bolt–flange in bearing [12]; ii) Bolt in shear [12]; iii) Bolt–connector bearing [12]; iv) CLT in local compression [13]; v) Dowel (screw) connection between connector and CLT [13]. For sake of brevity, references are provided for the codes used to determine the mechanical properties (stiffness and

strength) of these components. The assembly of these components allows the determination of the mechanical properties of the connection, namely, its stiffness and strength. The results of the analytical calculations (A.–New Connector) are compared with experimental tests in Fig. 9. Although the proposed analytical model is still preliminary, the comparison shows that the resistance of the connection is predicted with good accuracy. However, in terms of initial stiffness, the model underestimates the tests results. From the analytical model, a connection stiffness ($k_{10–40}$) of 168,7 kN/mm is obtained (see Table 3). Moreover, to assess the efficiency of the newly proposed connection, a comparison is made with a standard dowel-type connection consisting of two M16 bolts per side of the tested specimen. The mechanical properties of this latter connection are determined according to prEN 1995-1-1 [13], as it represents a typical dowel connection covered by the code. The chart clearly shows that the new connection is both stiffer and stronger. Specifically, for the material properties used in the experimental testing, the new shear connection is approximately 2,7 times stronger and 2,8 times stiffer than the traditional dowel-type connection.

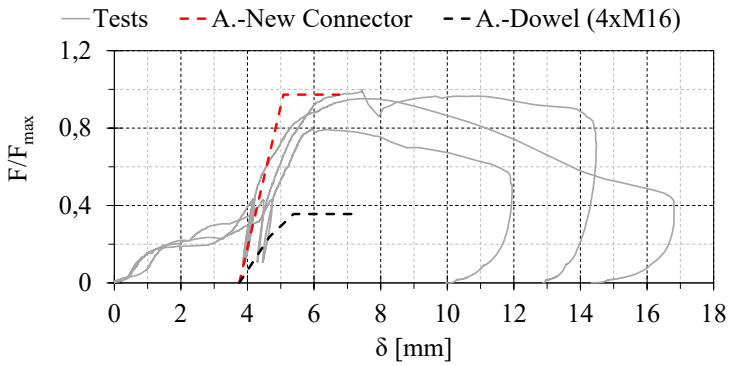

Fig. 9: Relative load-slip curves comparing analytical models with experimental results

6. Conclusions

The conclusions of this study are:

1. A newly designed disassembly shear connection for floor beams is presented, differing from common STC floor beam solutions in its load transfer mechanism.
2. Preliminary experimental results, including load–slip response, governing failure mode, and key mechanical properties, are reported and discussed.
3. A FEM numerical model is developed to reproduce the connection behaviour, and its accuracy is assessed against experimental results. Simulating wood requires a user-defined subroutine to capture its anisotropic behaviour, as the Hill yield criterion in Abaqus overestimates the connection's load capacity.
4. The component method is proposed to determine the mechanical response of the new connection; analytical predictions show good accuracy for strength, while stiffness is slightly underestimated.
5. Comparison with typical dowel-type connections demonstrates that both the strength and stiffness of the new connection outperform the conventional solution by a factor of approximately 2.7.

Finally, the shear connection presented in this paper is being investigated within the framework of the Research Foundation-Flanders (FWO) funded project CIRCOMP. As part of this project, ongoing research will further address long-term performance, reuse potential, and the bending behaviour of STC beams incorporating the newly developed shear connection.

Conflict of Interest

A patent application (EP25180501 on 03/06/2025) has been filed, covering the design and application of the described connector.

Acknowledgments

The authors acknowledge the financial support of the Research Foundation – Flanders (FWO) for the project CIRCOMP (SBO project S016424N).

References

[1] Loss C, Piazza M, Zandonini R. "Connections for steel–timber hy-brid prefabricated buildings. Part I: Experimental tests". Construction and Building Materials, Volume 122, 2016, Pages 781-795. (https://doi.org/10.1016/j.conbuildmat.2015.12.002)

[2] Hassanieh A, Valipour HR, Bradford MA. "Experimental and analytical behaviour of steel-timber composite connections". Construction and Building Materials, Volume 118, 2016,Pages 63-75. (https://doi.org/10.1016/j.conbuildmat.2016.05.052)

[3] Chiniforush AA, Valipour HR, Bradford MA, Akbarnezhad A. "Long-term behaviour of steel-timber composite (STC) shear connections". Engineering Structures, Volume 196, 2019, 109356. (https://doi.org/10.1016/j.engstruct.2019.109356)

[4] Romero A, Odenbreit C. "Experimental investigation on novel shear connections for demountable steel-timber composite (STC) beams and flooring systems". Engineering Structures, Volume 304, 2024, 117620. (https://doi.org/10.1016/j.engstruct.2024.117620)

[5] ECCS. "State of art on Steel-Timber-(Concrete) Structures". European Convention for Construction Steelwork, Publication N° 145, 1st Edition, 2024.

[6] Henriques J, De Ligne L, Degée H. "CIRCOMP – Developing a circular steel-timber composite floor system through innovative and demountable shear connections", SBO project S016424N, FWO – Research Foundation Flanders, 2024.

[7] COST. "Design of timber-concrete composite structures". A state-of-the-art report by COST Action FP1402 / WG 4, Shaker Verlag Aachen, 2018.

[8] EN 26891. "Timber Structures - Joints Made with Mechanical Fasteners - General Principles for the Determination of Strength and Deformation Characteristics". European Committee for Standardization (CEN), 1991.

[9] EN 1994. "Eurocode 4: Design of composite steel and concrete structures - Part 1-1: General rules and rules for buildings". European Committee for Standardization (CEN), 2005.

[10] Simulia D. Abaqus Documentation, 2024.

[11] Seeber F, Khaloian-Sarnaghi A, Yu T, Duddeck F, Van de Kuilen J-W. "Development and validation of an orthotropic 3D elasto-plastic damage model for wood, considering fiber déviations". Engineering Structures 308 (2024) 117928. (https://doi.org/10.1016/j.engstruct.2024.117928)

[12] CEN, European Committee for Standardization (2023) – "Eurocode 3: Design of steel structures – Part 1-8: Design of joints", FprEN 1993-1-8, October 2023, Brussels, Belgium.

[13] CEN, European Committee for Standardization (2025) – "Eurocode 5: Design of timber structures - Part 1-1: General rules and rules for buildings", FprEN 1995-1-1, April 2025, Brussels, Belgium.